tvst

Clinical Trials

Early Assessment of Circumferential Anterior Segment Structures Following Implantable Collamer Lens V4c Implantation Via SS-OCT

Fang Liu[1–3,*], Fei Xia[1–3,*], Lingling Niu[1–3], Jing Zhao[1–3], Xiaoying Wang[1–3], and Xingtao Zhou[1–3]

[1] Department of Ophthalmology and Optometry, Eye and ENT Hospital, Fudan University, Shanghai, China
[2] NHC Key Laboratory of Myopia (Fudan University), Key Laboratory of Myopia, Chinese Academy of Medical Sciences, Shanghai, China
[3] Shanghai Research Center of Ophthalmology and Optometry, Shanghai, China

Correspondence: Xingtao Zhou, Department of Ophthalmology and Optometry, Eye & ENT Hospital of Fudan University, No. 83 Fenyang Road, Shanghai 200031, China.
e-mail: doctzhouxingtao@163.com

Received: March 22, 2022
Accepted: September 27, 2022
Published: November 4, 2022

Keywords: circumferential anterior segment structure; implantable collamer lens V4c; swept-source optical coherence tomography

Citation: Liu F, Xia F, Niu L, Zhao J, Wang X, Zhou X. Early assessment of circumferential anterior segment structures following implantable collamer lens V4c implantation via SS-OCT. Transl Vis Sci Technol. 2022;11(11):4, https://doi.org/10.1167/tvst.11.11.4

Purpose: To explore early changes in circumferential anterior segment structures following Implantable Collamer Lens (ICL) V4c implantation via swept-source optical coherence tomography (SS-OCT).

Methods: In 103 eyes of 56 myopic patients undergoing ICL V4c surgery, anterior segments were measured via SS-OCT to compute local anterior chamber angle (ACA) parameters on the nasal–temporal (0°–180°), superior–inferior (90°–270°), and superior nasal–inferior temporal (80°–260°) meridians, including angle-opening distance at 500 µm (AOD500), trabecular–iris space area at 500 µm (TISA500), trabecular–iris angle at 500 µm (TIA500), and circumferential ACA parameters, including AOD area at 500 µm (AODA500), trabecular–iris circumference volume at 500 µm (TICV500), and the index and area of iris–trabecular contact (ITC). ACA parameters were compared preoperatively and at 1 week, 1 month, and 3 months postoperatively and compared among quadrants. Mixed-effects model was used to evaluate the parameters correlated with the post-ITC parameters.

Results: The mean AOD500, TISA500, TIA500, AODA500, and TICV500 were decreased by 65.4% to 71%, 64.1% to 69.3%, 53.8% to 61.5%, 69.9%, and 69.2%, respectively, at 1 week postoperatively. The ITC index and area values rose from 1.436% $\pm$ 4.427% and 0.070 $\pm$ 0.254 mm^2 to 12.343% $\pm$ 13.216% and 0.903 $\pm$ 1.304 mm^2 (all $P < 0.05$). No further decreases in ACA parameters were observed beyond 1 week postoperatively (all $P > 0.05$). Significant differences were observed among quadrants, with the narrowest in the superior–nasal quadrant, followed by the superior quadrant. The 3-month vault was significantly correlated with the ITC index and area at 3 months postoperatively.

Conclusions: Anterior segment structures were significantly shallow at 1 week with no further decreases thereafter. In light of anatomical variability, we recommend circumferential meridian scan to assess angle status, with special attention to the superior–nasal and superior quadrants.

Translational Relevance: We investigated the early changes in circumferential anterior segment structures following ICL V4c implantation, thus providing a better perspective for understanding anterior segment structural characteristics after ICL V4c surgery.

Introduction

Phakic posterior chamber implantable collamer lenses (ICLs) with a 0.36-mm central port have been widely employed for the correction of myopia, hyperopia, and astigmatism, improving vision while avoiding the need for iridotomy or iridectomy.[1–4] Due to its central port design, the ICL V4c (STAAR Surgical Company, Monrovia, CA) can maintain adequate aqueous flow. However, these lenses are also placed on the sulcus and share disadvantages with posterior

chamber ICLs, potentially resulting in complications including anterior chamber shallowing, pigment diffusion, cataract development, increased intraocular pressure (IOP), and the loss of endothelial cells.[5–8] Moreover, the vault, defined as the distance between the ICL posterior surface and the crystalline anterior surface, exhibits an ∼20% chance of being either too high (>1000 µm) or too low (<250 µm) as per standard online calculations from the manufacturer.[9,10] High vault has the potential to contribute to angle narrowing or the development of primary angle-closure glaucoma.[11] It is essential to evaluate the changes of anterior segment structure after ICL V4c placement.

In previous reports, researchers have documented inherent anatomical variability with respect to anterior segment structure in different meridian scans. However, most prior studies have only assessed anterior segment variability in horizontal meridian (temporal–nasal) images, thus potentially overlooking overall circumference status. Insufficient anterior chamber images may lead to the inaccurate judgment of angle closing or opening.[12] It is crucial to assess changes in 360° circumferential anterior chamber structures after ICL V4c surgery.

The CASIA2 (Tomey Corporation, Nagoya, Japan) represents a new generation of swept-source optical coherence tomography (SS-OCT) instruments. It offers a 16-mm-wide scanning range, and the 360° global scanning mode permits the simultaneous collection of images of the entire anterior chamber through 128 meridian scans with 256 angles. The present study was developed to assess early anterior chamber structures in angle-opening distance at 500 µm (AOD500), trabecular–iris space area at 500 µm (TISA500), and trabecular–iris angle at 500 µm (TIA500) in single cross-sectional scans of the nasal–temporal (0°–180°), superior–inferior (90°–270°), and superior nasal–inferior temporal (80°–260°) meridians, as well as AOD area at 500 µm (AODA500), trabecular–iris circumference volume at 500 µm (TICV500), and iris–trabecular contact (ITC) index and area in 360° circumferential scans following ICL V4c implantation, with the additional goal of identifying factors influencing the postoperative index and area of ITC.

Methods

Patients

This was a prospective, consecutive clinical study. In total, 56 patients between the ages of 20 and 38 years (103 eyes) were enrolled in the present study (23.21% male); four eyes of two patients were lost at the last follow-up. In total, 48 eyes were implanted with ICL V4c lenses and 55 eyes were implanted with toric ICL (TICL) V4c lenses at the Eye and ENT Hospital of Fudan University. The Ethics Committee of the Eye and ENT Hospital of Fudan University approved this study, and all procedures were consistent with the tenets of the Declaration of Helsinki. All patients provided written informed consent after being told about the study and potential associated risks.

Patient inclusion criteria were (1) age ≥18 years; (2) stable ametropia (progression ≤ 0.5 diopter [D] within 2 years); (3) anterior chamber depth (ACD) ≥ 2.8 mm (from the endothelium); (4) IOP < 21 mm Hg; and (5) endothelial cell density (ECD) ≥ 2500 cells/mm^2. Patients were excluded if they exhibited corneal dystrophy, suspected corneal ectasia, a history of ocular surgery/trauma, or a history of other ocular/systemic diseases.

Primary Refractive and Biometric Analyses

Standard ocular examinations were performed for all patients before and following surgery. Measured ocular parameters included (1) uncorrected distance visual acuity (UDVA), corrected distance visual acuity (CDVA), and manifest refractive error; (2) IOP; (3) white-to-white distance (WTW) and axial length (AL), determined using the ZEISS IOLMaster (Carl Zeiss Meditec, Wetzlar, Germany); (4) ECD (EM-4000; Tomey Corporation); (5) horizontal sulcus-to-sulcus diameter (STS); (6) slit-lamp and panoramic fundus photography; and (7) horizontal vault. Corneal topography and ACD were measured with a Pentacam HR (Oculus, Arlington, WA). Patient follow-up was conducted at 1 week, 1 month, and 3 months postoperatively.

CASIA2 SS-OCT Imaging

CASIA2 SS-OCT was used to evaluate patients in a dark room prior to contact-based examination. CASIA2 scans were conducted using a swept-source laser at a wavelength of 1310 nm, with 128 cross-sectional images being acquired in roughly 2.4 seconds. While applying minimal compression to the eyeball, the operator carefully pulled the upper and lower eyelids up and down, respectively, such that scanning of the entirety of the anterior segment structure could be performed. A 360° global scan analysis was then performed for all eyes after patients had focused on an internal target. The scleral spur (scleral protrusion inward corresponding to curvature changes at the corneoscleral junction)[13] was determined by two experienced operators, and

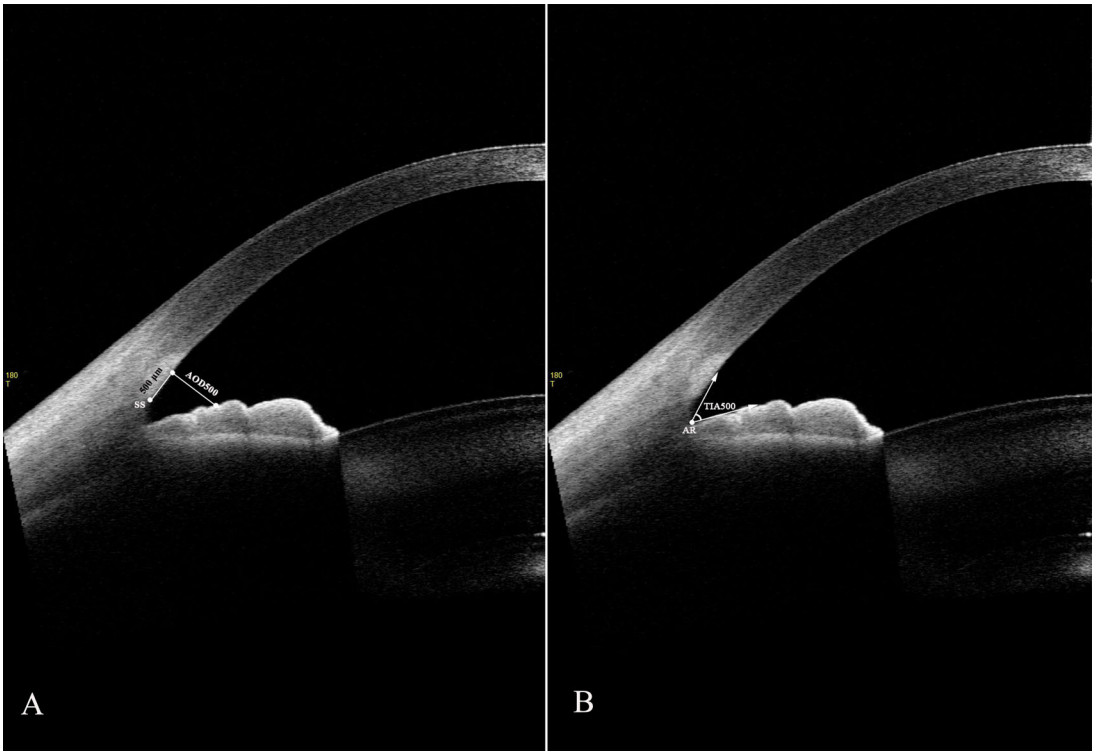

Figure 1. Two-dimensional anterior-segment OCT image exhibiting AOD500 (A) and TIA500 (B). AR, angle recess.

corresponding parameters were quantified automatically using the included software. Local anterior chamber angle (ACA) parameters were then computed from nasal–temporal (0°–180°), superior–inferior (90°–270°), and superior nasal–inferior temporal (80°–260°) meridian scans, with 360° circumferential ACA parameters being derived from 128 meridian scan images.

Local ACA Parameters

- Angle-opening distance at 500 µm (AOD500, µm), the perpendicular distance from the 500-µm anterior scleral spur to the anterior surface of the iris (Fig. 1A)[14]
- Trabecular–iris angle at 500 µm (TIA500, degree), the angle between a line from the 500 µm anterior

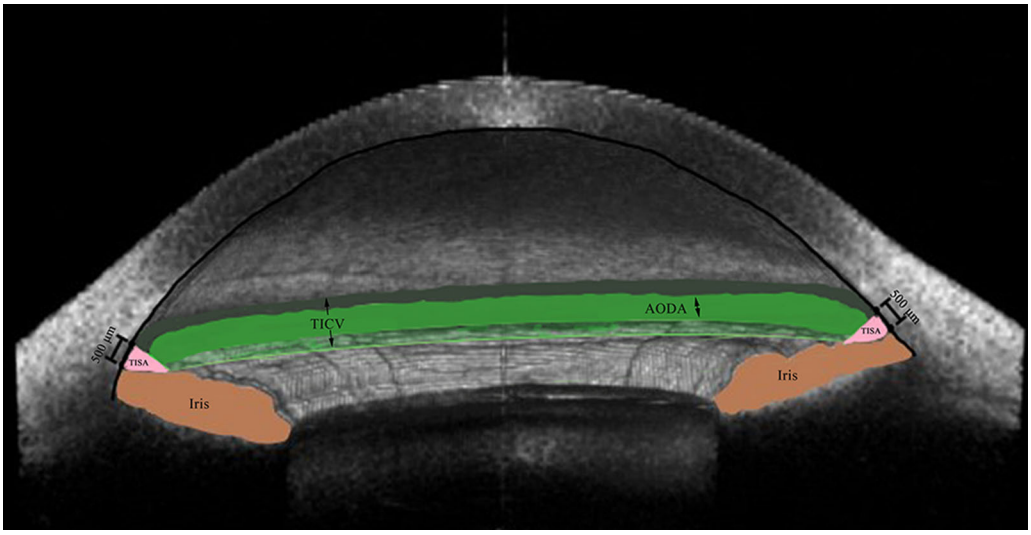

Figure 2. Three-dimensional anterior-segment OCT image exhibiting TICV500 (*arrow*; *dark green*, *green*, and *light green spaces*), AODA500 (*double-headed arrow*; *green space*), and TISA500 (*pink space*).

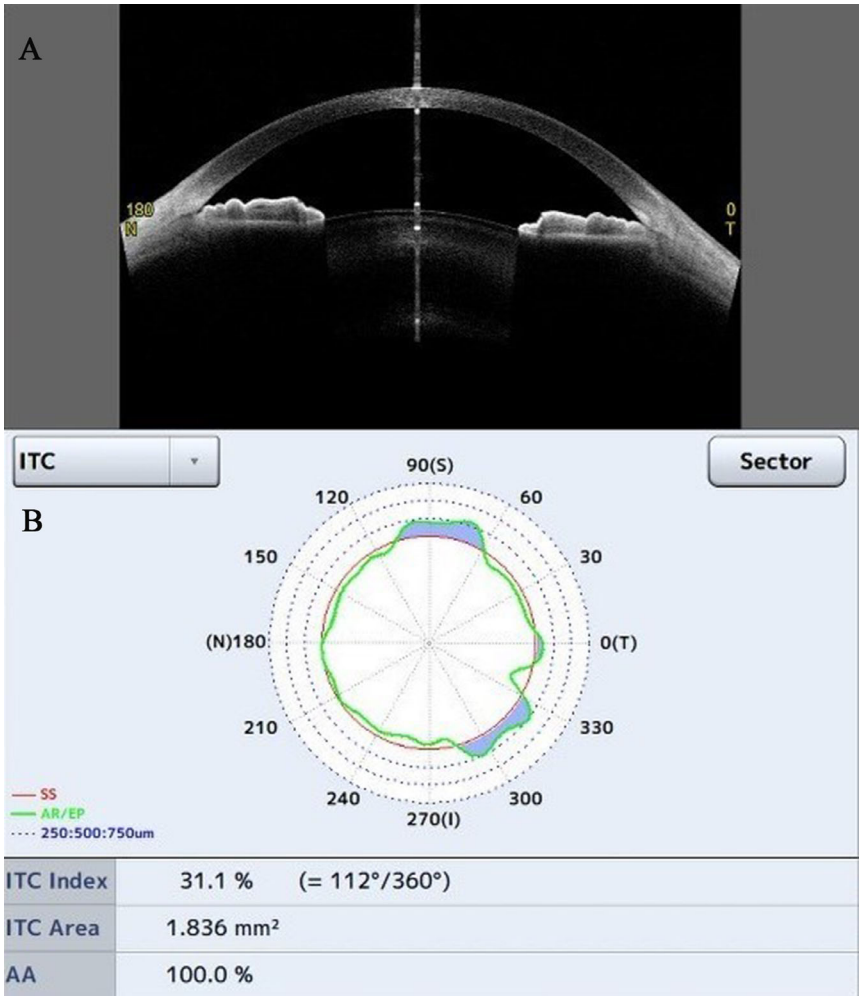

Figure 3. The ITC parameter analysis. (A) A cross-section image of the anterior chamber. (B) The chart shows the ITC index and area; the *blue area* indicates the amount and distribution of ITC.

angle recess toward Schwalbe's line and another line on the surface of iris crossing to the first line (Fig. 1B)

- Trabecular–iris space area at 500 µm (TISA500, mm^2), the trapezoidal area bordered by the AOD500, anterior surface of the iris, corneoscleral interface, and a vertical line from the scleral spur to the anterior iris surface (Fig. 2)[15]

360° Circumferential Parameters

- Angle-opening distance area at 500 µm (AODA500, mm^2), the composite area of the entire circumferential distance from AOD500 (Fig. 2)
- Trabecular–iris circumference volume at 500 µm (TICV500, mm^3), the composite volume of the entire circumferential area from TISA500 (Fig. 2)[16]
- Iris–trabecular contact index (ITC index, %), the degree of ITC existence (Fig. 3)[17]
- ITC area (mm^2), the composite area of the overall circumferential area from the length of contact between the iris and the corneoscleral wall (Fig. 3)

ICL/TICL V4c Surgical Procedure

ICL Power Calculation Software 3.0 (https://icl-power-calculation-software.software.informer.com/) used a modified vertex formula to determine the appropriate ICL/TICL V4c power. ICL/TICL size was calculated using previously measured WTW, STS, and ACD values. A single experienced surgeon (XZ) performed all surgical procedures. ICLs were horizontally implanted and TICL V4c implants were rotated less than 22.5° from the horizontal meridian to minimize rotation. Detailed surgical procedures were performed as in prior reports.[18] Postoperatively, patients were administered 0.1% topical prednisolone

acetate four times per day for 4 days, topical 0.5% levofloxacin four times per day for 7 days, and topical pranoprofen four times per day for 14 days.

Statistical Analysis

SPSS Statistics 20.0 (IBM, Chicago, IL) and SAS 9.4 (SAS Institute, Cary, NC) were used to conduct all statistical analyses. The normality of data distributions was assessed using the Shapiro–Wilk test. A mixed-effects model was used to compare differences in the quadrantal ACA parameters with Bonferroni adjustment, as well as an adjustment for binocular correlation to evaluate pre- and postoperative differences. Correlations among ITC index and area values, vault at 3 months, and preoperative factors that could affect anterior chamber status (sex, age, spherical equivalent [SE], ACD, AL, WTW, STS, intraocular lens size, pre-ITC index and area, AODA500, TICV500, mean AOD500, TISA500, and TIA500) were compared via rank correlation tests. Correlated factors ($P \leq 0.15$) were analyzed with a linear mixed-effects model to predict postoperative ITC index and area values. $P < 0.05$ was the threshold of significance.

Results

Efficacy and Safety

Surgical procedures were conducted successfully in all eyes without any intraoperative or postoperative complications during the 3-month follow-up period. Patient baseline demographic data are compiled in Table 1. The efficacy indices (postoperative UDVA/preoperative CDVA) and safety indices (postoperative CDVA/preoperative CDVA) were 1.14 ± 1.16 and 1.32 ± 1.18, respectively. All eyes exhibited a UDVA of 20/25, 95 eyes (96%) had a UDVA of 20/20 or better (Fig. 4A), and 94 eyes (95%) achieved a UDVA equal to or better than the preoperative CDVA (Fig. 4B). Relative to the preoperative CDVA, 47 eyes (47%) gained two Snellen lines, 12 eyes (12%) remained unchanged, and no eyes lost CDVA (Fig. 4C). Mean endothelial cell counts declined from preoperative values of 2756.51 ± 208.10 to 2654.9 ± 205.40 cells/mm^2 at 1 week postoperatively ($P < 0.001$), with no further reductions thereafter (all $P > 0.05$). There were no significant differences in IOP between pre- and postoperative values at any time point (all $P > 0.05$). At 3 months postoperatively, acceptable vault (250–750 µm) was evident in 76 eyes (76%), with values being significantly reduced from 688.78 ± 220.61 µm at 1 week to 636.28 ± 211.24 µm at 1 month and 615.97 ± 204.92 µm at 3 months (all $P < 0.05$) (Table 2). No pigment dispersion was found on the IOL surface in three following-up visits, as qualitatively evaluated by slit-lamp examinations.[19]

Table 1. Baseline Characteristics of 56 Patients (13 Male, 43 Female) After ICL (48 Spherical/55 Toric) or TICL V4c Implantation

Characteristic	Mean ± SD	Range
Age (y)	28.79 ± 4.35	20 to 38
AL (mm)	26.8 ± 1.44	22.91 to 30.99
SE (D)	−8.01 ± 2.56	−2.5 to −15.5
CDVA (logMAR)	−0.004 ± 0.022	0 to −0.18
ICL size (mm)	12.77 ± 0.36	12.10 to 13.20
ICL power (D)	−9.55 ± 2.68	−2.75 to −17.5
ACD (mm)	3.24 ± 0.23	2.76 to 3.76
STS (mm)	11.94 ± 0.39	10.81 to 12.66
WTW (mm)	12.02 ± 0.33	11.3 to 12.8

Predictability and Astigmatism Correction

In total, 88 eyes (88%) were within ±0.5 D of the target SE, and 98 eyes (99%) were within ±1 D (Fig. 4D). A scatterplot of the target and achieved SE values for all eyes is shown in Figure 4E. Postoperative astigmatism within half a diopter was evident in 74 eyes (74%), and 98 eyes (99%) were within ±1 D (Fig. 4F). Target induced astigmatism and surgically induced astigmatism vectors are shown in Figures 4G and 4H. Fifty-two TICL eyes (88%) exhibited an angle of error <±15°.

Changes in Local ACA Parameters

ACA parameters were assessed at baseline and at 1 week, 1 month, and 3 months postoperatively (Table 3). Relative to preoperative equivalents, AOD500, TISA500, and TIA500 values all decreased significantly after lens implantation (all $P < 0.01$), with no further decreases beyond 1 month (all $P > 0.05$). In the temporal, nasal, inferior, superior, inferior–temporal, and superior–nasal quadrants, corresponding mean AOD500 values declined at 1 week postoperatively by 71%, 66.9%, 66.4%, 70%, 65.4%, and 68.8%, respectively, with similar reductions being observed at 1 and 3 months postoperatively. Similarly, mean TISA500 and TIA500 values at 1 week postoperatively declined by 69.3%, 64.4%, 66.7%, 68.3%, 64.1%, and 66.6% and by 58.9%, 59.3%, 55.9%, 64.2%, 53.8%, and 61.5%, respectively. These reductions remained

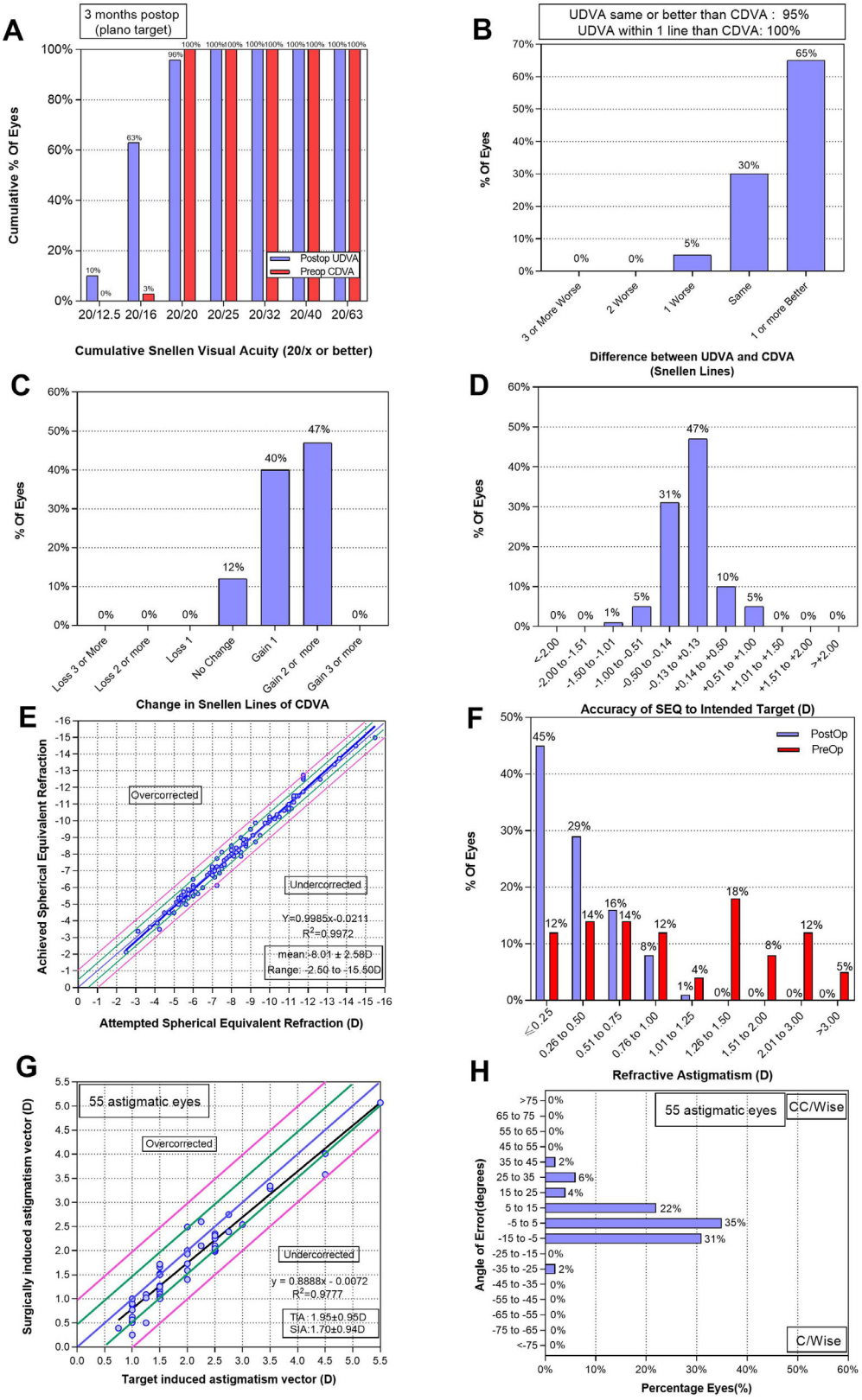

Figure 4. Refractive outcomes for 99 eyes at 3 months after placement of ICLs. (A) Cumulative UDVA; (B) postoperative UDVA versus preoperative CDVA; (C) changes in lines of CDVA; (D) SE refractive accuracy; (E) SE attempted versus achieved; (F) refractive astigmatism; (G) target-induced astigmatism versus surgically induced astigmatism after TICL; (H) refractive astigmatism angle of error after TICL.

Table 2. Biometric Parameters of 56 Patients Before and After ICL/TICL V4c Implantation

Parameter	Preoperative	1 Week Postoperative	1 Month Postoperative	3 Months Postoperative
IOP (mmHg)				
Mean ± SD	14.96 ± 2.17	13.68 ± 3.14	13.15 ± 2.14	14.09 ± 2.26
Range	10.9–20.4	8.8–26	9.3–20.7	9.9–20.3
ECD (cells/mm^2)				
Mean ± SD	2756.51 ± 208.10	2654.90 ± 205.40*	2690.31 ± 207.01	2715.68 ± 198.24
Range	2222–3253	2168–3171	2165–3135	2192–3263
Vault (µm)				
Mean ± SD	–	688.78 ± 220.61	636.28 ± 211.24[a]	615.97 ± 204.92[b]
Range	–	262–1180	262–1180	230–1113

[a]1 month postoperative versus 1 week postoperative, $P < 0.05$.
[b]Three months postoperative versus 1 month postoperative, $P < 0.05$.
*$P < 0.05$ versus preoperative.

stable for the remainder of the 3-month follow-up period. Significant differences were observed among quadrants at baseline and at the three follow-up time points (all $P < 0.01$). The local ACA parameter values tended to be lowest in the superior–nasal quadrant (80°), followed by the superior quadrant (90°).

Table 3. Changes in Local and Circumferential ACA Parameters (Mean ± SD) Before and 1 Week, 1 Month, and 3 Months After ICL V4c Implantation

Parameter	Preoperative	1 Week Postoperative	1 Month Postoperative	3 Months Postoperative
AOD500 (mm)				
Temporal	1.037 ± 0.332	0.301 ± 0.080*	0.279 ± 0.076*	0.288 ± 0.082*
Nasal	0.839 ± 0.250	0.278 ± 0.077*	0.282 ± 0.079*	0.291 ± 0.084*
Inferior	0.967 ± 0.331	0.326 ± 0.110*	0.323 ± 0.100*	0.329 ± 0.109*
Superior	0.792 ± 0.271	0.240 ± 0.082*	0.250 ± 0.089*	0.247 ± 0.089*
Inferior–temporal	0.903 ± 0.342	0.313 ± 0.108*	0.296 ± 0.092*	0.315 ± 0.106*
Superior–nasal	0.790 ± 0.265	0.246 ± 0.072*	0.238 ± 0.074*	0.245 ± 0.075*
P	<0.01	<0.01	<0.01	<0.01
TISA500 mm^2				
Temporal	0.369 ± 0.142	0.113 ± 0.033*	0.106 ± 0.033*	0.107 ± 0.034*
Nasal	0.301 ± 0.100	0.107 ± 0.031*	0.107 ± 0.031*	0.108 ± 0.034*
Inferior	0.359 ± 0.138	0.119 ± 0.040*	0.120 ± 0.040*	0.118 ± 0.039*
Superior	0.280 ± 0.117	0.090 ± 0.030*	0.088 ± 0.033*	0.088 ± 0.0.33*
Inferior–temporal	0.322 ± 0.140	0.116 ± 0.036*	0.110 ± 0.033*	0.114 ± 0.039*
Superior–nasal	0.276 ± 0.109	0.092 ± 0.024*	0.088 ± 0.028*	0.088 ± 0.029*
P	<0.01	<0.01	<0.01	<0.01
TIA500 (°)				
Temporal	61.541 ± 11.673	25.292 ± 6.189*	24.369 ± 6.476*	24.791 ± 7.459*
Nasal	58.648 ± 13.202	23.880 ± 5.916*	23.484 ± 5.849*	24.440 ± 6.700*
Inferior	56.543 ± 11.689	25.826 ± 8.662*	26.347 ± 7.615*	26.628 ± 8.419*
Superior	56.960 ± 11.789	20.380 ± 7.274*	21.757 ± 7.430*	21.389 ± 8.114*
Inferior–temporal	58.053 ± 12.583	26.829 ± 8.236*	24.956 ± 7.489*	26.063 ± 7.602*
Superior–nasal	56.161 ± 13.129	21.612 ± 7.428*	20.790 ± 7.026*	21.309 ± 7.361*
P	<0.01	<0.01	<0.01	<0.01
AODA500 (mm^2)	27.289 ± 8.123	8.225 ± 1.944*	8.519 ± 3.319*	8.507 ± 2.057*
TICV500 (mm^3)	9.666 ± 3.230	2.975 ± 0.798*	3.080 ± 1.260*	3.020 ± 0.850*
ITC index (%)	1.436 ± 4.427	12.343 ± 13.216*	12.890 ± 15.59*	13.754 ± 14.298*
ITC area (mm^2)	0.070 ± 0.254	0.903 ± 1.304*	1.060 ± 1.905*	1.077 ± 1.536*

*$P < 0.05$ versus preoperative.

Table 4. Correlation Analysis of Baseline Characteristics and Index and Area of ITC at 3 Months

	ITC Index			ITC Area		
Parameter	*r*	95% Confidence Interval	*P*	*r*	95% Confidence Interval	*P*
Sex[a]	−0.014	−0.218 to 0.191	0.89	−0.022	−0.225 to 0.183	0.833
Age (y)	−0.123	−0.319 to 0.083	0.227	−0.113	−0.310 to 0.093	0.269
SE (D)	−0.079	−0.279 to 0.127	0.44	−0.032	−0.234 to 0.174	0.758
ACD (mm)	0.12	−0.087 to 0.316	0.241	0.14	−0.066 to 0.334	0.17
AL (mm)	0.13	−0.076 to 0.326	0.201	0.101	−0.105 to 0.299	0.32
WTW (mm)	0.022	−0.186 to 0.227	0.835	0.067	−0.141 to 0.269	0.517
STS (mm)	−0.027	−0.233 to 0.182	0.797	0.018	−0.190 to 0.225	0.859
ICL size (mm)	0.032	−0.174 to 0.234	0.757	0.09	−0.116 to 0.289	0.379
ITC index, preoperative (%)	0.163	−0.048 to 0.361	0.118*	0.177	−0.034 to 0.372	0.091*
ITC area, preoperative (mm^2)	0.162	−0.049 to 0.360	0.12*	0.174	−0.037 to 0.370	0.095*
AODA500, preoperative (mm^2)	−0.083	−0.288 to 0.128	0.427	−0.077	−0.282 to 0.135	0.462
TICV500, preoperative (mm^3)	−0.162	−0.360 to 0.049	0.12*	−0.154	−0.353 to 0.057	0.139*
Mean AOD, preoperative (mm)	−0.029	−0.232 to 0.176	0.777	−0.031	−0.233 to 0.175	0.765
Mean TISA, preoperative (mm^2)	−0.089	−0.288 to 0.117	0.382	−0.084	−0.284 to 0.122	0.41
Mean TIA, preoperative (°)	0.008	−0.197 to 0.212	0.939	−0.008	−0.212 to 0.196	0.937
3-month vault (µm)	0.329	0.134 to 0.500	<0.001**	0.367	0.176 to 0.531	<0.001**

[a]Reference male.
*$P < 0.15$.
**$P < 0.05$, statistical significance.

Table 5. Multiple Linear Regression Analysis of Independent Factors Affecting the ITC Index and Area

Factor	β Coefficient	Standard Error	*P*
ITC index			
Intercept	8.775	6.044	0.153
Preoperative	−0.147	0.632	0.818
TICV, preoperative	−0.533	0.483	0.277
3-month vault	0.015	0.007	<0.05*
ITC area			
Intercept	0.366	0.541	0.502
Preoperative	−0.218	1.129	0.848
TICV, preoperative	−0.041	0.043	0.342
3-month vault	0.002	0.001	<0.05*

*$P < 0.05$, statistical significance.

Changes in 360° Circumferential Parameters

Postoperatively ITC index and area values rose from preoperative values of 1.436% ± 4.427% to 12.343% ± 13.216% and by 0.070 ± 0.254 mm^2 to 0.903 ± 1.304 mm^2, respectively, at 1 week postoperatively (all $P < 0.05$) (Table 3), with similar values at 1 and 3 months postoperatively. Conversely, AODA500 and TICV500 values were reduced by 69.9% and 69.2%, respectively, at 1 week postoperatively (all $P < 0.05$), and these values were similarly decreased by 68.8% and 68.1%, respectively, at 1 month postoperatively and by 68.8% and 68.8% at 3 months postoperatively.

Correlation analyses examining the relationships between ITC parameters and other factors were conducted next (Table 4). These analyses indicated that 3-month vault was positively correlated with both ITC index and area at 3 months postoperatively ($r_{\text{ITC index}} = 0.329$, $r_{\text{ITC area}} = 0.367$; all $P < 0.05$) (Fig. 2). These correlated parameters ($P \leq 0.15$) were then incorporated into a multivariate analysis designed to identify predictors of postoperative ITC area and index (Table 5). No relationship was found between preoperative SE and anterior segment parameters at 3 months (Supplementary Table S1). Also, there was no correlation between IOP and ITC index, ITC

area, or vault in the first week (Supplementary Table S2).

Because ITC index was significantly correlated with ITC area, one of these two parameters was included in the model. With respect to the ITC index at 3 months, only 3-month vault was significantly independently associated with this parameter (β coefficient = 0.015; $P < 0.05$). Similar findings were also observed with respect to ITC area (β coefficient = 0.002; $P < 0.05$). No other parameters incorporated into this analysis were independently associated with the examined ITC parameters.

Discussion

ICL V4c implantation has been widely performed to improve vision and associated quality of life in patients with a range of refractive errors. The central-hole design of these lenses markedly improves their utility and safety profile. Despite a reduced number of reported adverse events, anterior segment parameters remain important indicators when evaluating the safety of a given surgical procedure. This study was the first, to our knowledge, to have conducted a comprehensive assessment of circumferential and local anterior segment structure changes following ICL V4c placement. The safety and efficacy index values at 3 months postoperatively were 1.32 ± 1.18 and 1.14 ± 1.16, respectively; these results indicate that ICL V4c is safe and effective, consistent with our prior analyses.[18,20,21] We further found that 89% and 99% of eyes were within ±0.5 D and ±1 D, respectively, of the attempted SE, indicating good predictability and reliability with regard to correcting astigmatism. The primary result of our SS-OCT analysis was the observed shallowing of the circumferential and local anterior chamber structures at 1 week with no further decreases thereafter.

In line with these findings, several other researchers have observed a reduced angle width following ICL implantation. In 2009, Chun et al.[22] reported a 31.7% reduction in TIA500 (from 38.1° ± 8.7° to 26.0° ± 6.5°) and a 41.4% reduction in AOD500 (from 517.2 ± 180.2 μm to 302.8 ± 90.2 μm) at 1 month postoperatively when using ultrasound biomicroscopy, and they further found these decreases to be stable throughout the duration of a 2-year follow-up period. Moreover, Fernández-Vigo et al.[23] employed Fourier-domain OCT to detect reductions in mean TIA500, AOD500, and TISA500 values following ICL V4c surgery of 34.5% to 42%, 50.3% to 58.4%, and 46% to 59.2%, respectively, without any further reductions within 3 months postoperatively. The reductions in ACA parameters observed in the present study were greater than those in these prior reports, likely due to the different instruments employed and to higher baseline values in this study. In a separate analysis of patients with a shallow anterior chamber and lower baseline values, TIA500 and AOD500 values declined after surgery by 28.4% and 27.3%, respectively, further supporting our hypothesis. Following ICL V4c surgery, the narrowing of the anterior chamber width is associated with a higher risk of peripheral–anterior adhesion and/or angle-closure glaucoma. Prior studies have observed changes in anterior segment parameters no earlier than 1 month postoperatively, having failed to assess these changes at 1 week after ICL implantation. We observed no progressive shallowing of the anterior segment structures following the initial and pronounced narrowing that was evident at 1 week postoperatively. These results suggest that efforts should be taken to carefully monitor the anterior chamber structure and IOP in patients undergoing similar procedures, particularly during the first week after surgery.

In contrast to previous studies, we found that local ACA parameters differed significantly between quadrants at baseline and any follow-up time points. Although the ICL V4c was horizontally implanted in the sulcus, local ACA parameter values in the horizontal (0°–180°) meridian were not significantly lower than those in other quadrants. This may be attributable to the convex front of the lens resulting in the tent-effect–mediated 360° displacement of the iris in the pupil region. When using manual measurement approaches, Fernández-Vigo et al.[8] previously reported similar angle-width values (TIA500 and AOD500) in the nasal, temporal, and inferior quadrants. These different results may be attributed to our having utilized a new-generation SS-OCT that provides more detailed information pertaining to anterior segment structure in different quadrants. The semi-automated SS-OCT–mediated ACA parameter quantification improved substantially with respect to repeatability and reproducibility.[24,25] Xu et al.[12] reported that ranges and mean ACA parameter values measured in a single horizontal (temporal–nasal) meridian OCT image differed by 43.9% and 13.3%, respectively, from those obtained from 32 different meridian images. Based on these results, the authors posited that data derived from one or two OCT images may be insufficient to offer robust insight regarding potential anatomical variability with respect to angle-width parameters.

Porporato et al.[26] further reported that individual 80° to 260° SS-OCT scans exhibited the greatest degree of diagnostic performance compared to combinations of single horizontal scans (0°–180°) and vertical scans (90°–270°), diagonal scans (45°–225° and 135°–315°), or combinations of all four of these scans.

Our study observed shallower anterior segment structure in the superior (90°) and superior–nasal (80°) meridians, providing further evidence supporting the findings discussed above. Furthermore, the results offer important new insights into the evaluation of anterior chamber structures, as previous studies assessing changes in these studies conducted via anterior-segment OCT approaches were generally based on single horizontal OCT images and lacked a standardized approach to identifying OCT-based anatomical alterations. As our results emphasize, deeper anterior segment structures in horizontal meridian scans have the potential to lead to incorrect evaluation of angle status.

We then further employed a mixed-effects model in an effort to identify risk factors associated with postoperative ITC area and index values. After omitting factors not correlated with the ITC index at 3 months postoperatively ($P \geq 0.15$), a mixed-effects model incorporating the preoperative ITC index, ITC area, vault, and TICV500 was able utilized. The ITC index and area offer a general overview of the full 360° extent of the chamber angle closure based on SS-OCT scan findings. In prior reports, the ITC index was found to perform well when utilized to diagnose angle closure as detected via gonioscope (area under the curve = 0.83).[17] Relative to other angle parameters, ITC parameters are more closely associated with gonioscopy methods and can more readily explain the extent of angle closure. High vault values indicate greater tent-effect–mediated 360° displacement of the iris in the pupil with a shallower anterior segment structure. Although the ITC index and area values offered a valuable summary of the results of 128 cross-sectional OCT images, they were not sufficient to replace gonioscopy as a means of identifying synechial angle closure, instead serving as supplemental metrics.

The primary limitation of the present study is the relatively short follow-up period. Changes in anterior segment structures attributable to ICL placement should be further assessed over an extended period in a large patient cohort. Moreover, this study did not include eyes from hyperopic patients, who have the potential to exhibit a narrower chamber angle relative to that observed for myopic eyes. Vault values tend to decrease over time, so longer observation periods are important to assess the long-term safety of this procedure.

Conclusions

In summary, we observed significant anterior segment structure shallowing at 1 week postoperatively, and these changes remained stable over the entire 3-month postoperative period. We recommend that circumferential meridian scans be used to evaluate angle state, particularly in the superior–nasal and superior quadrants, which may be more prone to stenosis.

Acknowledgments

The authors thank to all of the patients for their participation and to the research staff at the Eye and ENT Hospital of Fudan University for their contributions to this study.

Supported by the National Natural Science Foundation of China (Grant No. 81770955), Joint Research Project of New Frontier Technology in Municipal Hospitals (SHDC12018103), Project of Shanghai Science and Technology (Grant No. 20410710100), Clinical Research Plan of SHDC (SHDC2020CR1043B), Project of Shanghai Xuhui District Science and Technology (2020-015), and Shanghai Municipal Commission of Health and Family Planning (202040285).

Disclosure: **F. Liu**, None; **F. Xia**, None; **L. Niu**, None; **J. Zhao**, None; **X. Wang**, None; **X. Zhou**, None

* FL and FX contributed equally to this work.

References

1. Siedlecki J, Schmelter V, Mayer WJ, et al. SMILE versus implantable collamer lens implantation for high myopia: a matched comparative study. *J Refract Surg*. 2020;36(3):150–159.
2. Sanders DR, Doney K, Poco M. United States Food and Drug Administration clinical trial of the Implantable Collamer Lens (ICL) for moderate to high myopia: three-year follow-up. *Ophthalmology*. 2004;111(9):1683–1692.
3. Packer M. Meta-analysis and review: effectiveness, safety, and central port design of the intraocular collamer lens. *Clin Ophthalmol*. 2016;10:1059–1077.
4. Packer M. The Implantable Collamer Lens with a central port: review of the literature. *Clin Ophthalmol*. 2018;12:2427–2438.
5. Zhao J, Zhao J, Yang W, et al. Peripheral anterior chamber depth and angle measurements using Pentacam after implantation of toric and non-toric implantable collamer lenses. *Front Med (Lausanne)*. 2021;8:610590.

6. Senthil S, Choudhari NS, Vaddavalli PK, Murthy S, Reddy JC, Garudadri CS. Etiology and management of raised intraocular pressure following posterior chamber phakic intraocular lens implantation in myopic eyes. *PLoS One*. 2016;11(11):e0165469.
7. Kamiya K, Shimizu K, Igarashi A, et al. Posterior chamber phakic intraocular lens implantation: comparative, multicentre study in 351 eyes with low-to-moderate or high myopia. *Br J Ophthalmol*. 2018;102(2):177–181.
8. Fernández-Vigo JI, Macarro-Merino A, Fernández-Vigo C, et al. Impacts of implantable collamer lens V4c placement on angle measurements made by optical coherence tomography: two-year follow-up. *Am J Ophthalmol*. 2017;181:37–45.
9. Lee DH, Choi SH, Chung ES, Chung TY. Correlation between preoperative biometry and posterior chamber phakic Visian Implantable Collamer Lens vaulting. *Ophthalmology*. 2012;119(2):272–277.
10. Nam SW, Lim DH, Hyun J, Chung ES, Chung TY. Buffering zone of implantable collamer lens sizing in V4c. *BMC Ophthalmol*. 2017;17(1):260.
11. Garcia-Feijoó J, Hernández-Matamoros JL, Castillo-Gómez A, et al. Secondary glaucoma and severe endothelial damage after silicone phakic posterior chamber intraocular lens implantation. *J Cataract Refract Surg*. 2004;30(8):1786–1789.
12. Xu BY, Israelsen P, Pan BX, Wang D, Jiang X, Varma R. Benefit of measuring anterior segment structures using an increased number of optical coherence tomography images: the Chinese American eye study. *Invest Ophthalmol Vis Sci*. 2016;57(14):6313–6319.
13. Ho SW, Baskaran M, Zheng C, et al. Swept source optical coherence tomography measurement of the iris-trabecular contact (ITC) index: a new parameter for angle closure. *Graefes Arch Clin Exp Ophthalmol*. 2013;251(4):1205–1211.
14. Pavlin CJ, Harasiewicz K, Foster FS. Ultrasound biomicroscopy of anterior segment structures in normal and glaucomatous eyes. *Am J Ophthalmol*. 1992;113(4):381–389.
15. Radhakrishnan S, Goldsmith J, Huang D, et al. Comparison of optical coherence tomography and ultrasound biomicroscopy for detection of narrow anterior chamber angles. *Arch Ophthalmol*. 2005;123(8):1053–1059.
16. Rigi M, Blieden LS, Nguyen D, et al. Trabecular-iris circumference volume in open angle eyes using swept-source Fourier domain anterior segment optical coherence tomography. *J Ophthalmol*. 2014;2014:590978.
17. Baskaran M, Ho SW, Tun TA, et al. Assessment of circumferential angle-closure by the iris-trabecular contact index with swept-source optical coherence tomography. *Ophthalmology*. 2013;120(11):2226–2231.
18. Wei R, Li M, Zhang H, et al. Comparison of objective and subjective visual quality early after implantable collamer lens V4c (ICL V4c) and small incision lenticule extraction (SMILE) for high myopia correction. *Acta Ophthalmol*. 2020;98(8):e943–e950.
19. Menezo JL, Peris-Martínez C, Cisneros AL, Martínez-Costa R. Phakic intraocular lenses to correct high myopia: Adatomed, Staar, and Artisan. *J Cataract Refract Surg*. 2004;30(1):33–44.
20. Wei R, Li M, Niu L, et al. Comparison of visual outcomes after non-toric and toric implantable collamer lens V4c for myopia and astigmatism. *Acta Ophthalmol*. 2021;99(5):511–518.
21. Zhao J, Zhao J, Yang W, et al. Peripheral anterior chamber depth and angle measurements using Pentacam after implantation of toric and non-toric implantable collamer lenses. *Front Med (Lausanne)*. 2021;8:610590.
22. Chun YS, Park IK, Lee HI, Lee JH, Kim JC. Iris and trabecular meshwork pigment changes after posterior chamber phakic intraocular lens implantation. *J Cataract Refract Surg*. 2006;32(9):1452–1458.
23. Fernandez-Vigo JI, Macarro-Merino A, Fernandez-Vigo C, et al. Effects of implantable collamer lens V4c placement on iridocorneal angle measurements by Fourier-domain optical coherence tomography. *Am J Ophthalmol*. 2016;162:43–52.e1.
24. Radhakrishnan S, Goldsmith J, Huang D, et al. Comparison of optical coherence tomography and ultrasound biomicroscopy for detection of narrow anterior chamber angles. *Arch Ophthalmol*. 2005;123(8):1053–1059.
25. Kim DY, Sung KR, Kang SY, et al. Characteristics and reproducibility of anterior chamber angle assessment by anterior-segment optical coherence tomography. *Acta Ophthalmol*. 2011;89(5):435–441.
26. Porporato N, Baskaran M, Perera S, et al. Evaluation of meridional scans for angle closure assessment with anterior segment swept-source optical coherence tomography. *Br J Ophthalmol*. 2021;105(1):131–134.